Thermal Machines Based on Surface Energy of Wetting: Thermodynamic Analysis

A. Laouir, L. Luo, D. Tondeur, T. Cachot, and P. Le Goff
Laboratoire des Sciences du Génie Chimique—CNRS, ENSIC-INPL, 54000 Nancy, France

This work proposes an original thermodynamic-energetic analysis of the feasibility and ideal performance of thermal machines based on the wetting phenomenon proposed by V. A. Eroshenko. The extension or contraction of a liquid film is taken as a "tutorial" example to introduce the basic thermodynamic relations of this 2-D transformation. It implies both mechanical and thermal effects, and this coupling allows conversion of heat to work (thermal engine) or conversely to pump heat (refrigeration/heat pump effect). A similar approach is then developed for the interface between a liquid and a highly microporous solid, having a large internal surface area. The thermodynamic behavior of this interface involves as state variables the surface tension of the liquid, the contact angle, and their dependence on temperature. Depending on the relative magnitude and sign of these quantities, and, therefore, on the working couple and the temperature range, a variety of machine cycles are feasible, or excluded, and a method is proposed for a comprehensive inventory. Order-of-magnitude calculations of the energy densities are presented based on the existing experimental data for several systems involving water as the fluid. The tentative conclusions are that the energy densities are very small on a mass basis compared to conventional systems based on vaporization, but the contrary is true on a volume basis because the phase transformation (extension of the surface) occurs in a condensed state. There may, therefore, be some niches for thermal machines of this type, but they remain to be identified and validated.

Introduction

During the 1990s, the Ukrainian physicist Valentin Eroschenko (Eroshenko, 1987, 1990, 1995, 1996; Fadeev and Eroshenko, 1997), promoted the idea that a solid–liquid interface could be considered as a working body in thermal machines, with potentially very interesting properties. Actually, his publications were preceded by a series of Soviet-Russian patents, originally classified, then partially unclassified, the first of which dates back to 1980 (Eroshenko, 1980, 1981, 1982, 1983, 1985, 1986, 1987).

Eroshenko's argument is that the work of expansion in machines based on vaporization is only a small part (say, 8%) of the energy of "dissociation" of the condensed phase, and that the energy density of the dilute vapor phase is small. On the other hand, a change in "dimensionality" of a condensed phase (such as going from a 3-D liquid to a 2-D liquid film) could imply high-energy density on a volume basis. These properties could be put to use in original devices for storing, transforming, or dissipating energy. In his series of articles and patents, Eroschenko proposed developing various mechanical devices, such as damping devices, mechanical-energy storage devices, actuators, and thermodynamic machines (engines, heat pumps, refrigerating machines), based on the use of interfacial energy of the wetting of a porous solid. These ideas gave rise to various research projects, mainly aimed at identifying efficient and convenient solid–fluid couples (Coiffard, 2001; Gomez et al., 2000). Some practical applications of purely mechanical devices were developed in the former Soviet Union, and a prototype of thermal engine allegedly developing power of 1 kW was built in Russia (Eroshenko, private communications). The technical details and the solid–fluid couple used have remained confidential.

The thermodynamic feasibility and the theoretical performances of such engines rely on the thermodynamic behavior of the solid–fluid working couple, expressed through the (σ,

Correspondence concerning this article should be addressed to D. Tondeur.

A, T) relationships, where σ denotes the surface tensions or the interfacial energy densities of the interfaces involved (solid/liquid/gas), and A denotes the interfacial areas involved. The (σ, A, T) relations in a sense here replace the (P, V, T) equation of state of the more conventional thermodynamic systems.

It is the purpose of the present article to give the inventory of, and to analyze the possible working cycles of such systems, described as thermodynamic cycles comparable to Carnot cycles, as a function of their (σ, A, T) behavior. The approach followed is essentially *energetic*, not mechanical (we consider heat and work, not forces), and quasi static (we ignore irreversibilities).

To illustrate the methodology of analysis, we introduce the simple example of a pure liquid film, that is, with just a liquid–gas interface and no solid present, for which the (σ, A, T) behavior is straightforward and the working cycle unique. The approach is then extended to a solid–fluid system, with three interfaces (solid–liquid, solid–gas, liquid–gas). Unlike the liquid-film case, a variety of behaviors will appear, giving rise to many possible working cycles, for engines as well as for heat or refrigerating pumps. These depend on the values of interfacial energies, on their dependence upon temperature, and on the thermicity of the wetting process. The latter criterion is used to construct a "state diagram," which allows a convenient classification of the feasible cycles. Those that appear to be of greater potential interest are considered in more detail, and some numerical examples, based on data in the literature, are presented.

Illustration: Liquid-Film Engine

Figure 1 shows a simple cycle of the liquid-film engine. The liquid film, a planar soap bubble, is formed on a rectangular wire frame, one side of which is mobile, so that the film can be stretched or contracted by moving this mobile side. The extension or contraction of the film obviously implies mechanical work, but an essential feature is that *it also involves heat*. The basic thermodynamic aspects presented below are essentially a reminder, because they are well known, and found in classic books on the subject (for example, Defay and Prigogine, 1951). We present them here because they are

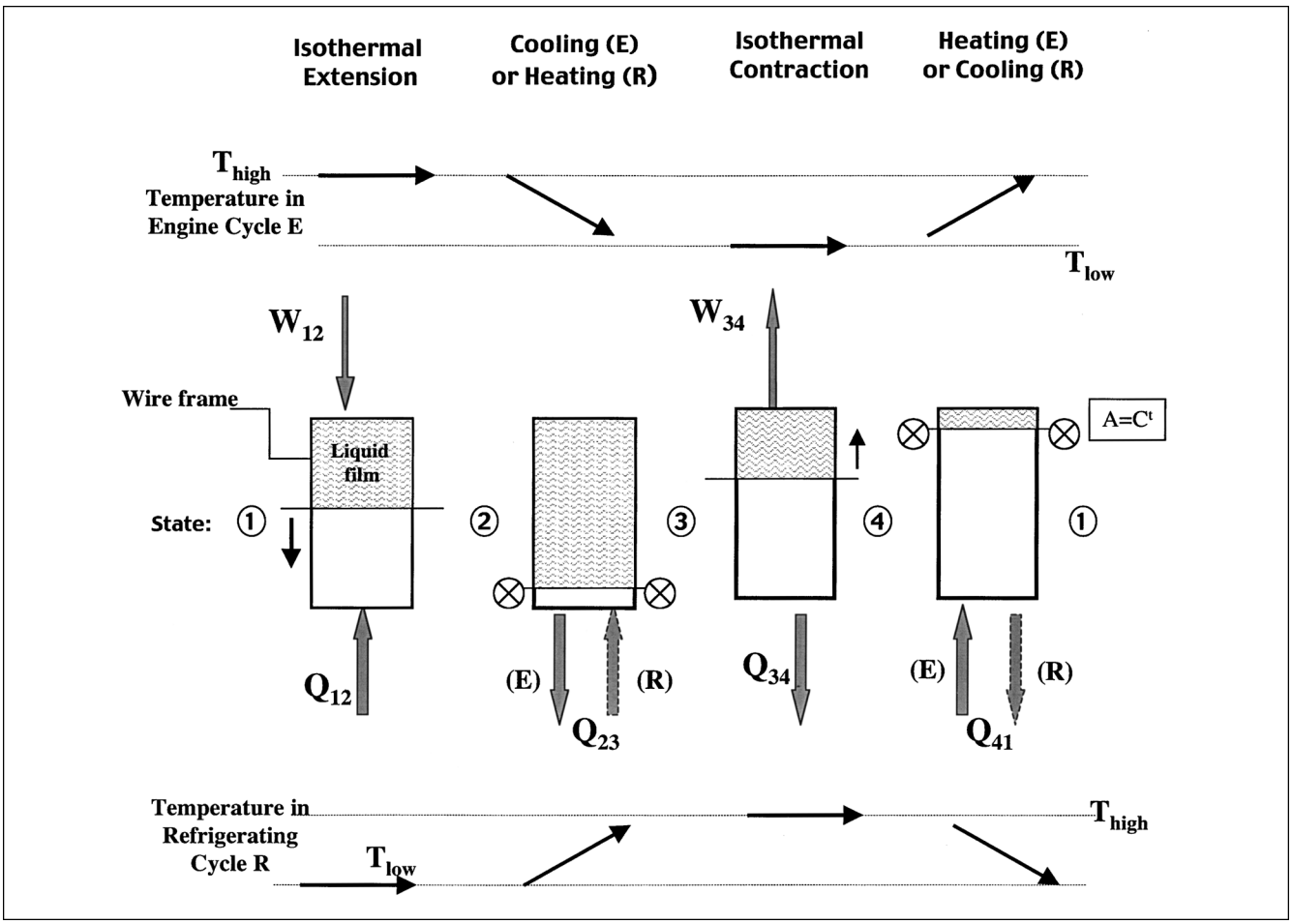

Figure 1. Liquid film machine.

The four steps of a Stirling-type cycle apply to both engine (E) and refrigerating or reverse (R) cycle. Only the temperature profiles (indicated on top and bottom) differ for engine and refrigeration cycles. States 1 to 4 are the starting or end states of each step and correspond to the couples of values of state variables shown in Figure 2. Fat arrows indicate the work or heat received or released by the system.

essential for the understanding of the less common analysis of thermal machines, and for the extension to solid–fluid systems, which we believe, involve some original aspects.

Thermodynamics of the film engine

Before analyzing this cycle, let us write down the basic thermodynamic relationships governing the extension or contraction. Considering that the film is a thermodynamic system with variables (U, S, A, T, σ), and U is a function of the extensive variables S and A, the Gibbs form of internal energy is

$$dU = TdS + \sigma dA \tag{1}$$

where σ is the interfacial energy density of the gas–liquid interface at the working temperature. It can be defined as the partial derivative of the internal energy of the film with respect to the interface area at constant entropy. In this formulation, the film is assumed to be incompressible in three dimensions. If this were not the case, the usual term in $-pdV$ would appear. The $+$ sign before σdA corresponds to the convention that the work done on the system for extension (for stretching the film) is positive, and σ is a surface *tension*, not a "spreading pressure." The two faces of the liquid film have to be considered as contributing to the surface area.

The conservation of energy during a transformation requires

$$dU = \delta Q + \delta W \tag{2}$$

The notation $\delta \boldsymbol{W}$ and $\delta \boldsymbol{Q}$ for work and heat *inputs* is used to recall that these quantities represent differentials of path-dependent quantities, and are not total differentials of state functions. We can then express the mechanical work of the extension as

$$\delta W = \sigma dA \tag{3}$$

In Eq. 1, dU being a total differential, the Maxwell relation applies to the partial derivatives, and is expressed as

$$\partial^2 U/\partial S \partial A = \partial^2 U/\partial A \partial S \tag{4}$$

or explicitly

$$(\partial T/\partial A)_S = (\partial \sigma/\partial S)_A \tag{5}$$

which in turn implies, for an isothermal transformation,

$$dS = -\, d\sigma/dT\, dA \tag{6}$$

The derivation of Eq. 6 from Eq. 5 is a simple manipulation of partial derivatives, developed in Appendix B. The surface tension is considered basically independent of the extension of surface A, and dependent only on T (Briant, 1989), hence, the ordinary derivative with respect to T. This is a major difference with P, V, T systems, and also with elastic 2-D systems like rubber balloons, where the interfacial energy density increases with an extension. Equation 6 furnishes an expression for the heat of isothermal extension

$$\delta Q = TdS = -\, T\, d\sigma/dT\, dA \tag{7}$$

The latter equation is known as Kelvin's equation (Briant, 1989; Moelwyn-Hughes, 1951; Thomson, 1859) and was established by him using a Carnot cycle, analogous to the cycle described below. An assumption is implied in this formulation, which we briefly recall, but without critical view, since it is not essential for the present purposes: it is assumed that the liquid film is in physicochemical equilibrium with the gas phase, that is, no evaporation or condensation takes place. Under these conditions, the nature of the gas phase has practically no effect on the interfacial energy, which can be assimilated to the surface tension of the pure liquid, a positive intrinsic quantity. From now on, we shall therefore refer to σ as the surface tension.

Surface tension generally decreases when temperature increases, and this dependence is usually described by power-law expressions (Guggenheim, 1945; Rowlinson and Widom, 1982; Weast and Astle, 1980; Reid et al., 1987)

$$\sigma = \sigma_0 (1 - T/T_c)^n$$

where T_c is the critical temperature of the liquid. The exponent $n = 11/9$ has been proposed for simple substances. For common pure liquids, a linear "equation of state" ($n = 1$) is suitable over a wide range of temperature and for many pure substances (Bernardin et al., 1997; Jasper, 1972)

$$\sigma = \sigma_0 - \alpha T \tag{8}$$

where α and σ_0 are two positive constants. A deeper study of these relationships can be followed using the Eötvös equation or the notion of parachor (Eötvös, 1886; Sudgen, 1930; Guggenheim, 1945; all quoted by Defay and Prigogine, 1951; Perry and Green, 1998). For our present purposes, we shall accept Eq. 8 and combine it with Eq. 7 to obtain

$$\delta Q = \alpha T\, dA \tag{9}$$

Equations 3 and 9 will be our working relations. Observe that if dA is positive (extension of the film surface), these two relations tell us that both δW and δQ (work and heat inputs into the system, thus furnished to the film) are positive. We shall say that the surface increase is *endomechanical* and *endothermal*. Let us again insist on the fact that *both faces of the liquid film* have to be considered when expressing the change in the surface area dA.

Ideal cycle of the film engine

Let us now investigate the cycle represented on Figure 1. We can call it a "Stirling cycle," because it comprises four steps completely analogous to this classic cycle: two isothermal surface changes, involving mechanical work and heat addition or removal, and two isosurface or "isochoric" temperature changes, involving heat exchange, but no mechanical-energy exchange. In addition, we shall see that the internal heat compensation can be considered between the isochoric steps in full analogy with a Stirling cycle.

Clearly, it would be possible to consider a Carnot cycle as well, composed of two isothermal steps as just given, and of two adiabatic steps of expansion or contraction. The reason for choosing a Stirling cycle here is that the heat and work involved are particularly simple to calculate, without requiring an "equation of state" to calculate the adiabatic steps. This choice does not change the feasibility, the qualitative behavior and the orders of magnitude involved.

In Figure 1, the four steps of the cycle that are given apply to both an engine, or direct cycle (noted E) and a refrigerating, or heat pump, or reverse cycle (noted R). Only the temperature profiles for the E and R cycles differ, and are shown in the top part and in the bottom part of the figure, respectively. The first step, from state 1 to state 2, is an isothermal extension (positive ΔA), occurring at the high temperature level of the cycle, T_h, and during which the work and heat inputs are

$$W_{12} = \sigma_h \Delta A \tag{10}$$

$$Q_{12} = T_h \alpha \Delta A \tag{11}$$

where $\Delta A = A_2 - A_1$, and σ_h is the value of the surface tension at that temperature. When referred to a unit mass of liquid, the heat input Q_{12} can be called the "isothermal latent heat of extension." Once the film is stretched to its maximum, the second step imposes a temperature decrease down to T_l; thus, the "input" of a *negative* quantity of heat Q_{23} corresponding to the thermal capacity C of the film is

$$Q_{23} = C(T_l - T_h) \tag{12}$$

The surface tension increases from σ_h to σ_l in this second step. The third step is an isothermal contraction occurring at the low temperature T_l, and releasing work and heat, to bring the film to state 4

$$W_{34} = -\sigma_l \Delta A \tag{13}$$

$$Q_{34} = -T_l \alpha \Delta A \tag{14}$$

Notice that we have replaced ΔA of Eqs. 10 and 11 by $-\Delta A$; in other words, we keep the definition of ΔA as $A_2 - A_1$, a positive quantity. Finally, the fourth step brings the system back to its initial state 1 by an isosurface heating from T_l to T_h involving a heat input

$$Q_{41} = C(T_h - T_l) \tag{15}$$

We have assumed that the thermal capacity, C, of the film is the same in its extended state and in its contracted state. This assumption is reasonable, but not essential to the present demonstration. It is clear that the *net work output* of the cycle is a positive quantity

$$W_{\text{net}} = -(W_{34} + W_{12}) = (\sigma_l - \sigma_h)\Delta A = \alpha(T_h - T_l)\Delta A > 0 \tag{16}$$

and the cycle is, therefore, that of a *heat engine*. By adding Eqs. 11 and 14, and neglecting the variation of the heat capacity, C, as just mentioned, we easily check that the *net heat input* is a positive quantity as well. In addition, the heat input Q_{12} is carried out at the high temperature of the cycle, in agreement with the second law.

Figure 2 presents three different diagrammatic representations of this Stirling cycle, in the (T, A), (T, S), and (σ, A) planes. The latter has the advantage of visualizing directly the net work furnished by the machine as the area of the rectangle (1, 2, 3, 4), just as in the (P, V) representation for conventional machines. The reader can easily reconstruct a Carnot cycle in such diagrams: a rectangle is obtained in the (T, S) diagram, whereas isentropic lines replace the vertical isosurface lines in the (T, A) and (σ, A) diagrams.

As in conventional machines, the efficiency is defined as the ratio of net work produced to heat input. Two cases can be distinguished here. In the first, we consider that the heat released during the cooling step is entirely recovered and used in the heating step. The only heat input to be considered in the efficiency then is that coming from the hot source Q_{12}. The efficiency is then equal to the thermal Carnot factor

$$\eta = W_{\text{net}}/Q_{12} = \alpha(T_h - T_l)/\alpha T_h = 1 - T_l/T_h = \eta_{\text{Carnot}} \tag{17}$$

The second case assumes no heat recovery and adds the additional heat Q_{41} to Q_{12} in the denominator. To express Q_{41} explicitly requires specifying the volume of liquid, or rather, the ratio of surface to volume, that is, the specific area a of the film. Explicitly, we obtain

$$1/\eta = (Q_{12} + Q_{41})/W_{\text{net}} = 1/\eta_{\text{Carnot}} + \rho C_p/(\alpha \Delta a) \tag{18}$$

where ρC_p is the volume-specific heat of the liquid and $\Delta a = \Delta A/V$ is the difference in specific area of the film between its extended and its contracted states. The quantity

$$\Lambda = \rho C_p/(\alpha \Delta a) \tag{19}$$

is a nondimensional number that characterizes the ratio between sensible heat of the liquid and latent heat of extension, in other words, between volume energy and surface energy. Obviously, we would like this number to be as small as possible, to have an efficiency as close as possible to the reversible Carnot value. We shall evaluate orders of magnitude further below.

From heat engine to heat pump

Having designed a heat engine, it is straightforward to design a heat pump or a refrigerating machine using the same film system. We know that this amounts to reversing the direction of rotation in the operating diagrams of Figure 2, for example, turning clockwise instead of counterclockwise in the (σ, A) diagram. It also implies that there is a net input of mechanical energy into the system, and that the heat input, Q_{12}, during extension has to be done at the low temperature, T_l (cooling effect), while the heat release during contraction must occur at the high temperature, T_h (heat pump effect). The succession of steps is that of cycle R in Figure 1.

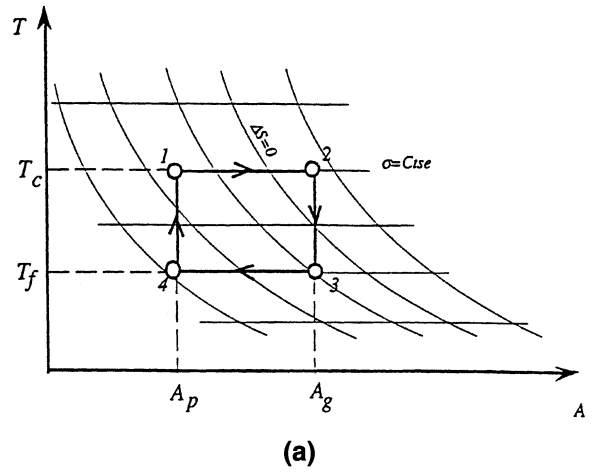

(a)

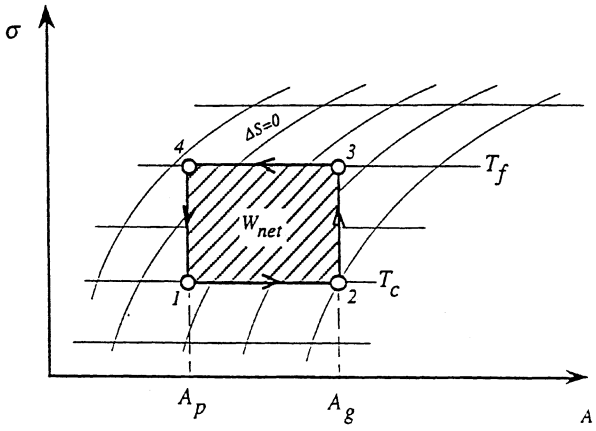

(b)

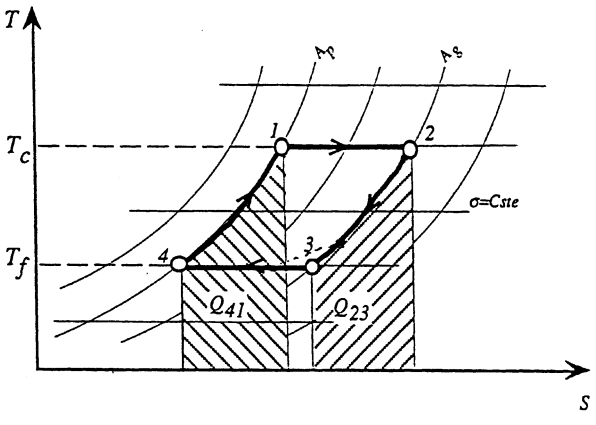

(c)

Figure 2. Thermodynamic diagrams of the liquid film for an engine cycle.

Points 1, 2, 3, 4 represent the four states in Figure 1; (a) temperature vs. area with constant entropy contour lines; (b) surface tension vs. area with constant entropy contour lines; the area in the rectangle measures the net work output of the engine cycle; (c) temperature vs. entropy with constant area contour lines.

It is customary to characterize the performance of "reverse thermal machines" by a coefficient of performance (COP). If, for example, we consider that it is a cooling cycle, the "cold COP" is defined as the ratio of the heat removed from the cold source to the net work input, $W_{12} + W_{34}$ (recalling that these quantities are algebraic). If the cooling step 41 can be compensated by the heating step 23, the heat removed from the cold source is Q_{12} and the COP is that of an inverse Carnot cycle

$$\text{Cold COP}_{\text{rev}} = Q_{12}/[W_{12} + W_{34}] = T_l/(T_h - T_l) = T_l/(T_h \eta_{\text{Carnot}}) \quad (20)$$

Without internal compensation, the cooling duty Q_{41} must be furnished by the cold source and subtracted from Q_{12}

$$\text{Cold COP} = \text{cold COP}_{\text{rev}} - \Lambda \quad (21)$$

where Λ is given by Eq. 19. Classically, if we consider that the cycle is a heat pump rather than a cooling machine, the "hot COP" is defined as the ratio of the heat given to the hot well $|Q_{34}|$ to the net work input, and is equal to the cold COP augmented by 1. Without internal compensation, the quantity $|Q_{23}|$ must be subtracted from $|Q_{34}|$, and it is found that the form of Eq. 21 remains unchanged, while "cold COP" is replaced by "hot COP."

Orders of magnitude

Table 1 summarizes for three common liquids—water, mercury, and ethanol—some values of surface tension, σ, at two temperatures; of the temperature coefficient, α, of surface tension; and of the physical properties entering the Λ number, and also of the latent heat of vaporization. The behavior of ethanol is more or less typical of organic liquids and that of mercury is typical of liquid metals; water is as we know, a peculiar substance. The data are gathered from Perry and Green (1998) and Weast and Astle (1985). For the specific surface variation, Δa, we have taken 10^9 m^2m^{-3}, which corresponds to a film with a thickness of 1 nanometer, considered for both its faces, and reduced by half during contraction. This value has also been conserved for the systems involving solids, and we shall discuss it further in this context. We emphasize this point because the numerical values are very dependent on this value, which is chosen such that the surface energy is on the same order of magnitude as the volume energy, but we see that this requires a very high state of division in the liquid. From these data, we calculated the heat and work corresponding to each step of the refrigerating cycle of Figure 1. The values are contained in Table 2.

The following comments can be made:

- The heat of vaporization is one order of magnitude larger than the total energy of extension $W + Q$ for all three liquids. This result can be compared to the values of the so-called Stefan ratio (Stefan, 1886; Defay and Prigogine, 1951, chap. 11) usually contained between 2 and 8. Actually, for the Stefan ratio to be valid, one should probably extend the film to the thickness of one molecule, or about 5 or 10 times greater than considered here.
- This observation might, at first sight, appear to limit applications. However, a different view is obtained when one

Table 1. Physical Properties of Three Liquids

Liquid	σ at 0°C ($J \cdot m^{-2}$)	σ at 50°C ($J \cdot m^{-2}$)	α ($J \cdot m^{-2} \cdot K^{-1}$)	ρ $kg \cdot m^{-3}$	C_p $J \cdot kg^{-1} \cdot K^{-1}$	Λ	ΔH_{vap} $kJ \cdot kg^{-1}$
Water	75.8×10^{-3}	67.9×10^{-3}	0.16×10^{-3}	1,000	4,180	26	2,445
Mercury	490.6×10^{-3}	480.4×10^{-3}	0.20×10^{-3}	13,500	140	9	292
Ethanol	24.0×10^{-3}	19.9×10^{-3}	0.08×10^{-3}	789	2,440	24	900

compares the energy content per unit volume, and considers that in machines based on vaporization and condensation, most of the volume is occupied by vapor. For water, the volume energy density, ρQ_{12}, of the liquid film is of the order of 50 kJ per liter. For water vapor at 5 bars and 25°C, the density is approximately 4 g/L, giving an energy density for vaporization of about 10 kJ per liter of vapor. On this volume basis, it is seen that the energy density is highest for the liquid film. There is, thus, some potential for compactness in surface-energy machines! Another comparison is with the potential energy of liquid water stored for hydraulic energy, recalling that 1 kg of water falling by 1 m in a gravity field corresponds to only 9.81 J.

- The sensible heat for heating (Q_{23}) or cooling (Q_{41}) the fluid is also considerably larger than the latent heat of extension! This makes efficient internal recuperation a necessity for any machine of this type, if energetic performances are sought.
- A reversible cooling cycle with perfect recuperation, working between 0°C and 50°C will give a cold COP_{rev} of $273/50 = 5.46$, independent of the fluid. On the other hand, the values given in the last column of Table 2 are calculated from Eq. 20 using the W and Q values in the table. It can be seen that the maximal deviation from the theoretical value is smaller than 5%. The corresponding hot COP_{rev} of a heat pump would be equal to 6.46.
- The values of the nondimensional number Λ are clearly larger than the values of the COP. Obviously from Eq. 21, without internal recuperation, the COP would be negative, making it a very inefficient machine indeed! This would be all the more true, the lower the specific surface factor, Δa.
- The corresponding efficiency of the reversible engine cycle (Stirling or Carnot) is $50/323 = 0.155$. Applying Eq. 18, without internal recuperation, gives efficiencies of 0.03, 0.06, 0.033, respectively, for water, mercury, and ethanol. These values are not ridiculous compared to the Carnot efficiency, but it should be kept in mind that, except for internal recuperation, they still concern ideal, reversible machines!

Partial conclusion

These semiquantitative evaluations are not very favorable for efficient energetic performances of thermomechanical machines based on pure liquid films. The maximum (reversible) efficiency is of course equal to the Carnot factor, thus determined by the upper and lower temperatures of the cycle, and necessarily small around the near-ambient temperatures envisaged here. As to the energy density, the prognosis is interesting if one considers the criterion of energy per unit volume of working fluid.

These machines may have other interesting features not investigated here, like working under mild conditions with low-grade energy. However, the purpose of this exercise was not to advocate such machines, but to set the stage for investigating fluid–solid systems. For this reason, we first have to extend the preceding thermodynamic approach to these systems.

Thermodynamics of Wetting Machines

In the following, we now introduce a solid–liquid interface, and we call *wetting process* the extension of this interface, and *dewetting process* the opposite process. The wetting process of a solid surface by a liquid can be considered in two ways, depending on the presence or absence of a liquid–gas interface, and the thermodynamic equations are somewhat different, as established below. A very clear, thorough, and comprehensive presentation of the thermodynamics of wetting can be found in Rouquerol et al. (1999), together with methods to measure the thermodynamic quantities.

Wetting nonporous solid surfaces

First consider the quasistatic spreading of a large liquid film on a flat surface, as shown on Figure 3. There are three interfaces—solid–liquid, solid–gas, liquid–gas—with corresponding interfacial energy densities σ_{sl}, σ_{sg}, and σ_{lg}, the latter being the surface tension of the liquid introduced earlier. The equilibrium situation of the film is described by the well-known Young equation (Young, 1805), resulting from a balance of forces at the ternary interface, as shown on Figure 3, which also introduces the contact angle, θ

$$\sigma_{lg} \cos \theta = \sigma_{sg} - \sigma_{sl}. \tag{22}$$

The magnitude of the contact angle, or more conveniently, of its cosine, is classically a measure of the "wetting strength" of

Table 2. Work and Heat for Each Step of the Heat Pump Cycle (R) of Figure 1*

	Step 1-2		Step 2-3		Step 3-4		Step 4-1		COP
	W_{12}	Q_{12}	W_{23}	Q_{23}	W_{34}	Q_{34}	W_{41}	Q_{41}	Calculated
Water	75.8	43.7	0	209.0	−67.9	−51.7	0	−209.0	5.53
Mercury	36.3	4.0	0	7.0	−35.6	−5.0	0	−7.0	5.71
Ethanol	30.4	27.7	0	122.0	−25.2	−32.7	0	−122.0	5.33

*Values are in kJ per kg of liquid.

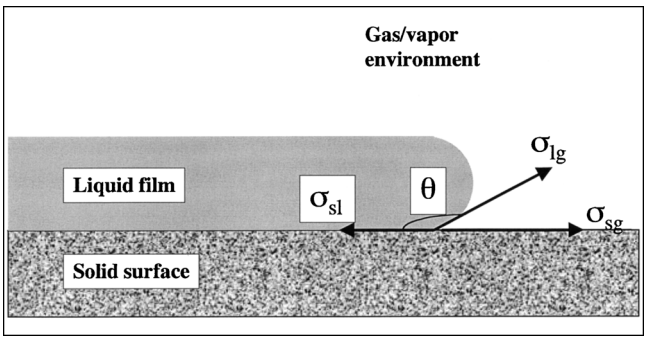

Figure 3. Equilibrium of an extended liquid film on a solid surface.

the liquid with respect to the solid. The smaller θ is, the larger cos θ, and the stronger the wetting. When θ becomes larger than 90°, as in Figure 3, that is, when cos θ becomes negative, we have "weak wetting."

Considering again that the system is 3-D incompressible, the Gibbs equation governing changes is an extension of Eq. 1, which we write

$$dU = TdS + \Sigma \sigma_i dA_i \tag{23}$$

The index i stands for the three different interfaces. When the liquid spreads as a film, the solid–liquid interface and the liquid–gas interface both extend, essentially by the same amount, while the solid–gas interface shrinks by the same amount. Equation 23 therefore can be rewritten

$$dU = TdS + (\sigma_{sl} + \sigma_{lg} - \sigma_{sg})dA \tag{24}$$

where dA denotes the variation of the solid–liquid interface. Substitution of Eq. 22 into Eq. 24 eliminates the interfacial energies of the solid with the gas and the liquid (they are actually condensed into the contact angle), to yield

$$dU = TdS + \sigma_{lg}(1 - \cos\theta)dA \tag{25}$$

We should keep in mind that the physics of wetting considered here are somewhat simplified with respect to modern knowledge: the notion of contact angle introduced here is a static notion, the dynamic advancing and receding angles may be different; there may exist a very thin precursor film extending well beyond the "macroscopic" film (De Gennes, 1985, for example); and Young's equation is somewhat problematic, especially in view of the heterogeneity of surfaces (Neumann, 1974). We shall nevertheless consider that the classic notions, on which Young's equation is based, are acceptable for present purposes, and under the assumption of quasi static evolutions.

Wetting porous solids

Let us now consider the second type of wetting process, without the liquid–gas interface. This essentially occurs when porous solids with a high surface area per unit volume are used. In experiments analogous to the mercury porosimeter, the liquid is originally contained in a closed vessel, with a negligible gas–liquid interface, and is pumped into the porosity of the solid. Thus, initially there is a solid–gas interface, replaced at the end of the process by an equivalent solid–liquid interface. The liquid is in contact with gas only along a porous cross section of the solid, which is essentially constant, so that the variation of this interface is in any case negligibly small. In Eq. 24, the term σ_{lg} is, therefore, absent, and Eq. 25 subsequently reduces to

$$dU = TdS - \sigma_{lg}\cos\theta dA \tag{26}$$

Although there is no liquid–gas interface, the surface tension of the liquid appears explicitly, because the quasi static displacement is still governed by Young's equation. Equation 26 rather than Eq. 25 will be our working equation, since we are interested in systems with high interfacial areas, that is, in porous solids. Heretofore, we let $\sigma_{lg} = \sigma$ since the liquid surface tension will be the only such term to appear.

The derivation going from Eq. 2 to Eq. 7 is then repeated, with $+\sigma$ replaced by $-\sigma\cos\theta$. The new forms of Eqs. 3 and 7 are then simply

$$\delta W = -\sigma\cos\theta dA \tag{27}$$

$$\delta Q = TdS = -T\partial(-\sigma\cos\theta)/\partial T dA \tag{28}$$

With both σ and θ considered to depend on temperature only, the latter equation will be designated the "modified Kelvin equation," and may be rewritten as

$$\delta Q = T[(d\sigma/dT)\cos\theta - \sigma(d\theta/dT)\sin\theta]dA \tag{29}$$

Equations 27 and 29 are our working equations for studying thermodynamic cycles. Notice that earlier work (Eroshenko, 1997; Coiffard, 2001) neglects the dependence of the contact angle on temperature, that is, the second term on the righthand side of Eq. 29. We shall see that on the contrary this term plays a fundamental role in the thermal behavior, and, therefore, in the cycle performances.

First consider the sign of the work requirement δW. For weak wetting behavior, cos θ is negative, and the work of wetting is positive, that is, the wetting process (the extension of the liquid–solid interface) is endomechanical (it requires work input into the system) the same as the extension of the pure liquid film. On the other hand, it is exomechanical for strong wetting behavior, that is, when $\cos\theta > 0$. We shall denote the endomechanical or exomechanical character of the process by the term "mechanicity." Note that if one considers the system globally (liquid + solid + gas) as a compressible medium, undergoing a macroscopic volume change dV under pressure P, the resulting work $-PdV$ is equal to that given by Eq. 27.

The heat of wetting suggests more complex behavior, since δQ depends not only on α and θ, but on their temperature derivatives as well. The dependence of θ on temperature may be relatively complex and not necessarily monotonous. We shall designate the endothermal or exothermal character of the process by the term "thermicity." It will prove convenient to represent all the possible situations on the diagram that we introduce in the next section.

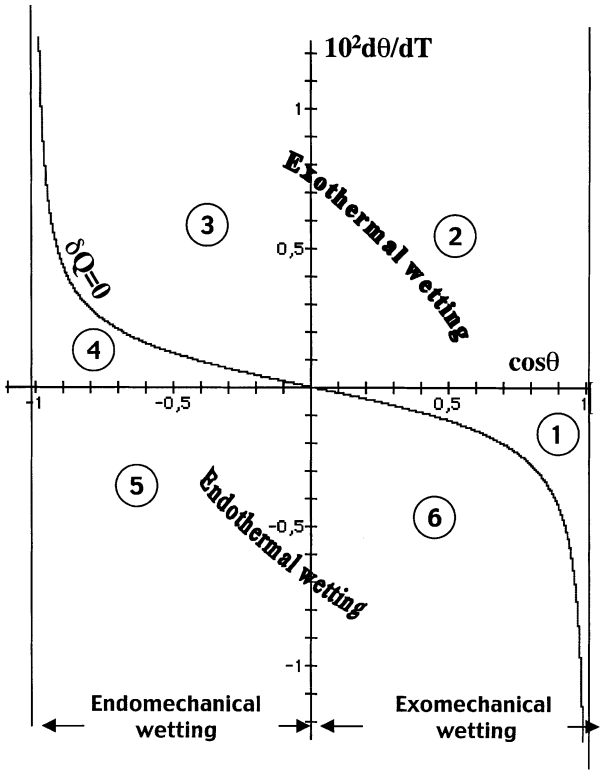

Figure 4. Thermicity–mechanicity diagram of the wetting process.

The two axes and curve $\delta Q = 0$ divide the plane into zones numbered 1 to 6, which differ by at least one of the criteria thermicity, mechanicity, and sign of $d\theta/dT$.

Thermicity–Mechanicity Diagram of Solids Wetting

Figure 4 is a plot of $d\theta/dT$ vs. $\cos\theta$. Using these coordinates, we represent the curve $\delta Q = 0$ (athermicity curve) constructed from Eq. 29, taking for σ and $d\sigma/dT$ the values for water at 0°C. It is easy to verify that if a linear $\sigma(T)$ relation is assumed (Eq. 8), this curve has an algebraic equation of the form

$$y = -Bx/\sqrt{(1-x^2)} \tag{30}$$

where $y = d\theta/dT$, $x = \cos\theta$, and $B = \alpha/\sigma$. It is symmetrical with respect to the origin, where it has a slope equal to $-B$. The parameter B contains the physical properties intrinsic to the liquid, and, thus, depends on the temperature (it has the dimension of an inverse temperature). For water at 0°C and 50°C, the values of B are 0.0021 and 0.0024 K^{-1}, respectively, and the two curves are hardly distinguishable. For our present purposes, we shall therefore consider that there is a unique athermicity curve. The following features of the diagram can be put forward:

- Above the horizontal axis, θ increases with temperature, and decreases below.
- On the right of the vertical axis ($\cos\theta > 0$) there is strong wetting behavior and the wetting process is exomechanical ($\delta W < 0$); on the left of the vertical axis, there is weak wetting behavior and the wetting process is endomechanical ($\delta W > 0$).

Table 3. Thermicity and Mechanicity of the Wetting Process in Different Zones of Figure 4

Zones	1	2	3	4	5	6
Thermal	Exo	Exo	Exo	Endo	Endo	Endo
Mechanical	Exo	Exo	Endo	Endo	Endo	Exo

- Above the $\delta Q = 0$ line, the wetting process is exothermal ($\delta Q < 0$); below this line, it is endothermal ($\delta Q > 0$).

These properties can be checked easily from Eq. 29, keeping in mind that $d\sigma/dT = -\alpha$, and that the curve $\delta Q = 0$ is hardly affected by temperature in the range 0°C to 50°C. Six zones are determined by these lines. Temperature is a parameter (it should actually be plotted on a third axis in a 3-D representation). Changing the temperature of a given system may switch the behavior from one zone to another.

Table 3 summarizes the mechanical and thermal behavior in the six zones for the wetting process. Dewetting, of course, exhibits the opposite properties. We notice that from the point of view of thermicity and mechanicity behavior, zones 1 and 2 on the one hand, and zones 4 and 5 on the other hand, have the same behavior. We emphasize that we are considering quasi static processes, that is, processes with no irreversibilities. It is clear that, for example, the rapid forced intrusion of a nonwetting liquid into a porous medium can be accompanied by strong frictional dissipation. Such irreversible phenomena can well offset and mask the exomechanical and/or endothermal character of the quasi static process.

Thermodynamic Cycles of Wetting-Based Machines

If we consider that each of the two working temperatures of a cycle can correspond to anyone of the zones, then there are $6 \times 6 = 36$ possible couples of zones, and, therefore, *a priori* 36 different cycles. If in addition all these 36 cycles can be run either as an engine cycle or as refrigerating/heat pump cycle, then there are 72 possible cycles. Not all of these are realistic and/or of practical interest. Our purpose is not to describe them all, but rather to eliminate impossibilities and classify the possible behaviors.

We first eliminate all cycles that would violate the second law of thermodynamics by having *both the wetting and the dewetting steps endothermal.* No heat rejection would then take place, and this obviously makes engine cycles impossible, by virtue of the second law, in its Carnot formulation: a thermal engine requires a hot source and a cold well. The reverse machines—refrigerators/heat pumps—require a cold source and a hot well, and are also impossible with this cycle. Indeed, a simple entropy balance on such a cycle shows that entropy would accumulate in the machine incompatibly with a cyclic regime.

Next, we consider the "duals" of the previous cycles, in which *both the wetting and dewetting steps exothermal.* Since the machine does not absorb heat (except for the compensated temperature change), no cooling/heat pump effect is possible, and no engine cycle is possible (no heat intake that can be transformed into work). Since the entropy output during a cycle is obviously positive, no reversible cycle is possible, and the corresponding machine would just degrade part of the mechanical work input into heat, and restore another

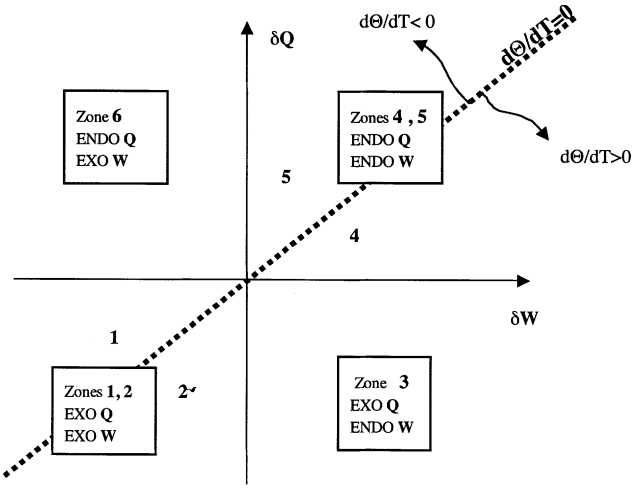

Figure 5. Different representation of the thermicity–mechanicity diagram.

EXOQ means exothermal wetting; ENDOW means endomechanical wetting, for example. Zones 4 and 5 correspond to the behavior of the simple liquid film.

part (temporary storage function). Such a machine is not ruled out by thermodynamics, and may be of use for storage purposes, but it is of no interest for the present purpose.

Combining the two preceding restrictions requires that the zones of wetting and dewetting conditions are on the same side with respect to the $\delta Q = 0$ curve and reduces the number of cases by half.

A further restriction can be introduced by imposing *exomechanical dewetting*, implying that the dewetting process should occur spontaneously. If this were not the case, there would be a practical difficulty in separating the liquid from the solid if the latter is microporous. The capillary pressure is likely to be so high that vacuum pumping, for example, will achieve no result (except for partially vaporizing the liquid). Only high-pressure displacement can be considered, but this is highly inefficient and inconvenient when the displacing fluid is a gas. Therefore, we want $\cos\ \theta < 0$ during this process. This restricts the operating region to zones 3, 4, and 5 of Figure 4 for the dewetting step.

Combining these constraints results in the following configurations for the operating conditions of the wetting and dewetting steps:

A: wetting and dewetting in zone 4 or 5;
B: wetting and dewetting in zone 3;
C: wetting in zone 6 and dewetting in zone 4 or 5;
D: wetting in zone 1 or 2 and dewetting in zone 3.

Since zones 4 and 5 have the same thermicity and mechanicity, they can be considered for the time being as one and the same zone from the point of view of thermodynamic cycles. The same is true for zones 1 and 2. We shall see later that the sign of the derivative $d\theta/dt$ plays an important role, and we therefore keep track of it. For the present, the basic cases are summarized in Table 4.

It appears appropriate to introduce a new representation, in which the relationship between thermicity and mechanicity appears in a more straightforward manner, but where the contact angle is no longer used as a coordinate element. Figure 5 shows a δQ vs. δW diagram. The straight line along which $d\theta/dT = 0$ is shown, with the temperature-dependent slope equal to $-T/B = 1 - \sigma_0/\sigma$. This property can be derived by solving Eq. 29 for $d\theta/dT$ as a function of δQ and δW, and equating it to zero. In this new representation, the six zones of Figure 4 are determined by this straight line and the four quadrants of the diagram. The thermicity and mechanicity of the *wetting process* have been indicated.

Table 4. Basic Cases for Wetting Machines

Cycle	Zones	Step	Thermicity	Mechanicity
A	4 or 5	Wetting	Endo	Endo
	4 or 5	Dewetting	Exo	Exo
B	3	Wetting	Exo	Endo
	3	Dewetting	Endo	Exo
C	6	Wetting	Endo	Exo
	4 or 5	Dewetting	Exo	Exo
D	1 or 2	Wetting	Exo	Exo
	3	Dewetting	Endo	Exo

Examples with Physical Systems

Although a considerable amount of data on "isothermal" contact angles are available (Zisman, 1964; Jasper, 1972; Vold and Vold, 1983; Pepin et al., 1998; Gomez, 2000; Hansen et al., 2000; Good and Yu, 2001; Coiffard, 2001), the data on its dependence on temperature are very scarce. The experimental couples considered below are based on data of Neumann (1974). More data can be found in Bernardin (1997) and De Ruijter et al. (1998). The data used here are represented graphically in Appendix A for three couples. The values of heat, Q, and work, W, have been calculated with a specific surface area of 10^9 m^2m^{-3}, the same as for the liquid film.

Table 5 gives a sample of calculation results effected on both engine and refrigeration cycles, and intended to give orders of magnitude. The values of Q and W of the fourth and fifth columns refer to the refrigerating step in a cooling cycle of type A and B, as described below. Thus, Q is a measure of the cooling capacity. On the other hand, the values of W_{net} in the last column refer to an engine cycle, and are calculated as the difference between the work output in the exomechanical step and the work input in the endomechanical step. All these values are obtained using Eqs. 27 and 29, together with the physical parameters in Tables 1 and 5.

Cycle A

Now consider as a first example an engine cycle corresponding to conditions A, thus occurring entirely in Zone 5, the wetting process being both endothermal and endomechanical. The operating cycle is qualitatively that of Figure 1, with the temperature profile indicated in the top part. The reverse cycle, giving a refrigeration/heat pump, is schematically the same, but with the temperature profile reversed (indicated in the bottom part of the figure). These two cycles are represented with a different physical symbol in Figure 6. The wetting step, that is, the extension of the liquid–solid interface corresponds to the intrusion of liquid into the pores.

Table 5. Contact Angles and Energy Exchanged During Cycles Between 0°C and 50°C for Three Systems of Neumann

	θ at 0°C (Deg/Rad)	$d\theta/dT$ (Rad·K^{-1})	Cycle Zone	Q^* at 0°C (kJ·kg^{-1} Water)	W^{**} at 0°C (kJ·kg^{-1} Water)	$W_{net}{}^{\dagger}$ (kJ·kg^{-1} Water)
Water/cholesteryl acetate	103.4°	-2.3×10^{-4}	A	$Q_{12}=14.7$	$W_{12}=+17.6$	2.6
	1.804		5			
Water/hexatria contane	102.6°	$+17.4\times10^{-4}$	B	$Q_{34}=25.6$	$W_{34}=-16.5$	4.0
	1.791	3	3			
Water/siliconed glass	106.3°	$+8.7\times10^{-4}$	B	$Q_{34}=5.0$	$W_{34}=-21.3$	0.6
	1.855		3			

*Q is the heat removed from the cold source at 0°C in a cooling cycle (calculated from Eq. 29).
**W is the work given to the system during the same cold step (calculated from Eq. 27).
†W_{net} designates the net work produced by an engine cycle (given by Eq. 16).

The refrigeration effect is produced during this wetting step. A possible couple with this behavior is water/cholesteryl acetate (see the curve in Figure A3 in Appendix A, and Table 5).

Cycle B

The conditions are that of Zone 3, and the wetting process is exothermal and endomechanical. The engine cycle and the refrigeration cycle are shown on Figure 7. In contrast to the preceding, the wetting step is exothermal, and must occur at a low temperature for an engine cycle and at a high temperature for the refrigeration cycle. Possible couples are water/siliconed glass, and water/hexatriacontane (hydrocarbon in C36) (see the curves in Figures A1 and A2 in Appendix A, and Table 5).

The following comments are appropriate:

- The cooling capacity is very small *on a weight of fluid basis*, even smaller than for pure liquid-water film. On the other hand, *on a volume of fluid basis*, the 14.7 or the 25.6 kJ·L^{-1} water compare interestingly with the 10 kJ·L^{-1} water vapor of a system based on vaporization.

- For the water/cholesteryl acetate system, the two contributions to the expression of δQ (Eq. 29) have the same (positive) sign, because of the negative sign of $d\sigma/dT$, of cos θ, and of $d\theta/dT$. From the point of view of the cooling capacity, it is, therefore, interesting to have both large negative values of $d\theta/dT$ and large values of $\theta > 90°$, thus, to be far from the

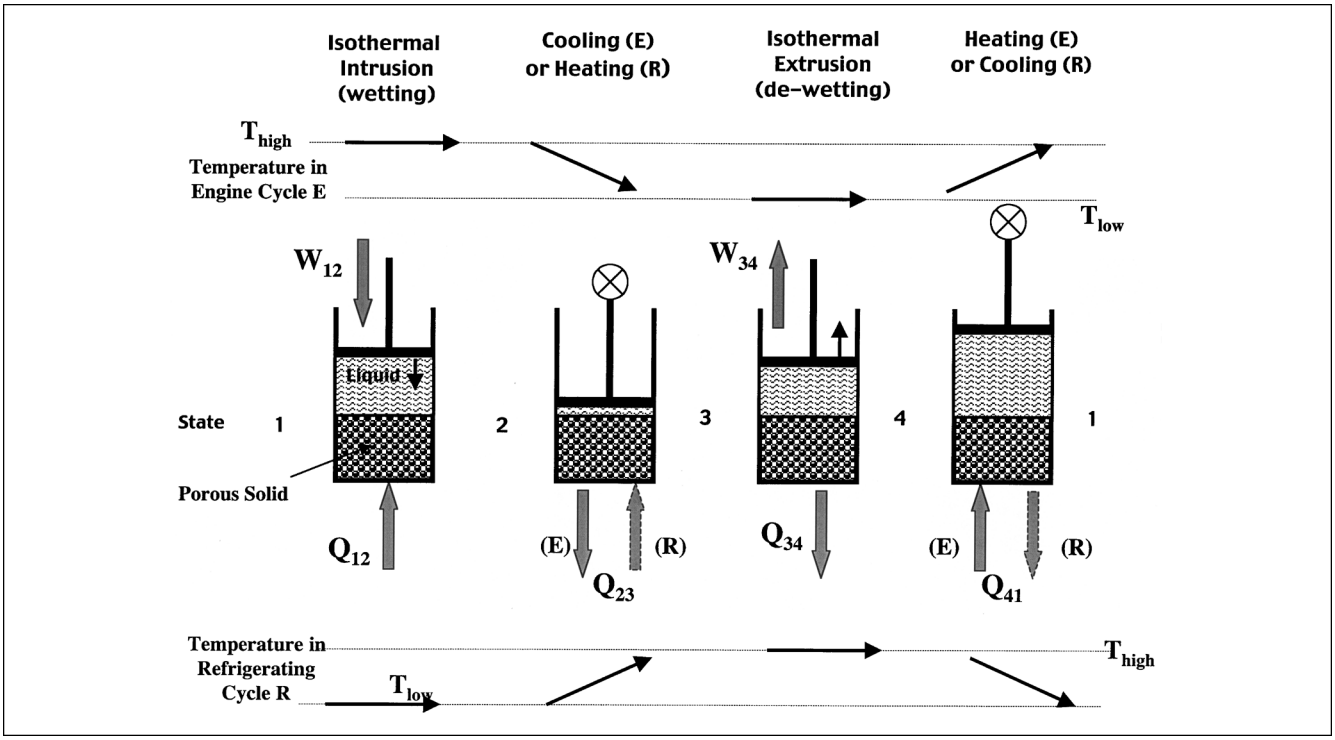

Figure 6. Wetting machine cycles for Cycle A.

The porous medium is symbolized by little balls. The wetting process (first step of the cycle) is symbolized by the downward movement of the piston, forcing intrusion of the liquid into the pores. Fat grey arrows symbolize heat and work received or released by the system. The only difference between engine cycle (E) and refrigeration cycle (R) is in the temperature profile (indicated on the top and bottom).

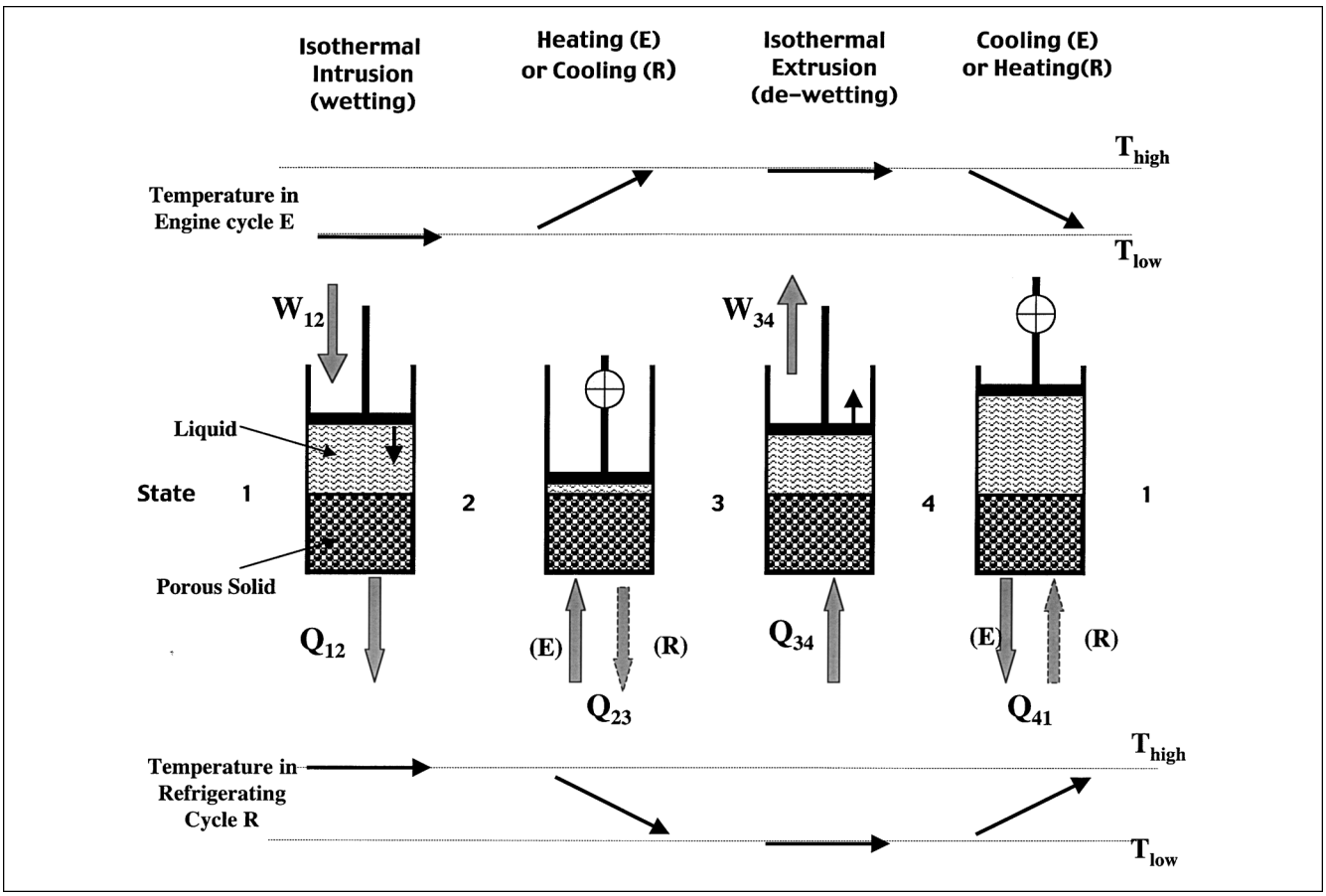

Figure 7. Wetting machine cycles for Cycle B.

With respect to Cycle A, note the difference in the temperature profiles, and in the direction of heat arrows.

origin in Zone 5. We call this situation *synergistic for refrigeration*.

• For the two other systems (cycle B), the two contributions to δQ are of the opposite sign, and the second contribution dominates. We call this situation *antagonistic for refrigeration*. It is advantageous to have large positive values of $d\theta/dT$, and small values of cos θ, and, thus, a contact angle as close to 90° as possible at the cold temperature of the cycle; the first contribution would then tend to vanish, and the net work would be of the order of $|W|$ given in column five of Table 5, and the cooling capacity would be, respectively, of the order of 36 and 18 $kJ \cdot kg^{-1}$ water.

• The net work for the engine cycle is calculated by combining Eqs. 16 and 27; thus

$$W_{net} = -(W_{34} + W_{12}) = |\Delta(\sigma \cos\theta)| \cdot \Delta A \qquad (31)$$

where Δ stands for the difference in the conditions of the two isothermal steps, and, thus, at the two temperature limits of the cycle. This net work is very small indeed, smaller than that of the pure water film ($|W_{12} + W_{34}| = 7.9$ $kJ \cdot kg^{-1}$ from Table 2).

• For the water/cholesteryl acetate system, the change of both σ and $|\cos\theta|$ with temperature is in the same direction (cos θ increases, but being negative, its absolute value decreases), and the two effects are thus *synergistic for engine*. This is why the net work output for this system is relatively large in view of the small temperature sensitivity of the contact angle. For the two other systems, the effects of the variation of σ and $|\cos\theta|$ are antagonistic; this reduces the effect of the relatively high temperature sensitivity of the contact angle for the water/hexatriacontane pair.

• For these reasons, increasing the temperature interval for the water/cholesteryl acetate system improves the performance, although not by a large factor; for example, if we took the more favorable interval (40–70°C), we would obtain a net work of 2.9 $kJ \cdot kg^{-1}$, and if we extrapolated the data linearly to 100°C, we would obtain 5.5 $kJ \cdot kg^{-1}$ (see Figure A3 in Appendix A for the data). On the other hand, increasing the temperature interval for the other two systems (cycle B) hardly changes the figures, because the decrease in the surface tension of water offsets the increase in the contact angle when temperature increases.

As a partial conclusion, no spectacular result is to be expected from the particular systems at hand, even at slightly different temperature intervals. The best performing system among the three, both from the point of view of cooling capacity and work output, is water/hexatriacontane, which has the largest variation of contact angle and the value closest to 90° (where the variation of the cosine is most sensitive to the

variation of the angle). Nevertheless, the qualitative behavior of the water/cholesteryl acetate system seems more promising because of the synergistic effects mentioned. We should therefore search for a system having the same qualitative behavior as water/cholesteryl acetate, but quantitatively much more sensitive to temperature, and with a stronger hydrophobic character (larger contact angle). Alternately, systems like water/hexatriacontane may be interesting if the contact angle is close to 90° at the cold temperature of the cycle.

Other cycles

We shall discuss the other cases more briefly, because we currently have no experimental example available that has the appropriate properties. It is nevertheless valuable to examine these properties because, as we shall see, different thermodynamic behaviors appear, and some appear impossible or impractical.

Cycle C. The conditions of the wetting step are that of Zone 6 (endothermal, exomechanical), and the conditions of dewetting are those of Zone 4–5 (exothermal, exomechanical). *Both the wetting and dewetting steps produce mechanical work*, which makes it a very interesting situation for an engine cycle. Besides finding an appropriate pair, several aspects need to be discussed before one can hope to take full advantage of this. Let us merely summarize here the essentials without demonstration:

- An engine cycle is possible (as that shown on Figure 8) providing the contact angle decreases upon heating, in agreement with $d\theta/dT$ being negative in Zones 5 and 6.
- A refrigerating cycle is impossible if the dewetting conditions are in Zone 5, and possible if they are in Zone 4, but only with a particular and hypothetical nonmonotonous variation of the contact angle. It seems that practically, *we can rule out refrigeration/heat pump cycles of type C*.
- For the engine cycle, it would be interesting to have a large variation of the contact angle that is symmetric about 90°. For example, with a 5° variation, the net work would be about 6.3 $kJ \cdot kg^{-1}$ of water (compare this with the values in Table 5), but it would be about 50 $kJ \cdot kg^{-1}$ for a 40° variation, a value still small compared with the vaporization energy on the basis of weight, but considerable on the basis of volume.

Cycle D. The conditions are those of Zone 1–2 for wetting (exothermal, exomechanical), and Zone 3 for dewetting (endothermal, exomechanical). This situation is comparable to that of Cycle C, in the sense that *we have two exomechanical steps*. For the engine cycle, the endothermal dewetting step must be done at a high temperature, and, therefore, the contact angle must increase when the temperature increases, from Zone 2 to Zone 3, in agreement with the sign of $d\theta/dT$ in these zones. On the other hand, for the same reasons as stated earlier for Cycle C, one can show that the refrigeration/heat pump cycles are practically ruled out under conditions D. The engine cycle is shown on Figure 9.

Cycles with Nonspontaneous Dewetting. Finally, we comment briefly on the situations where the wetting and dewetting conditions are in the same zone, but with "unfavorable," that is, nonspontaneous dewetting, that is, $\cos\theta > 0$. We keep

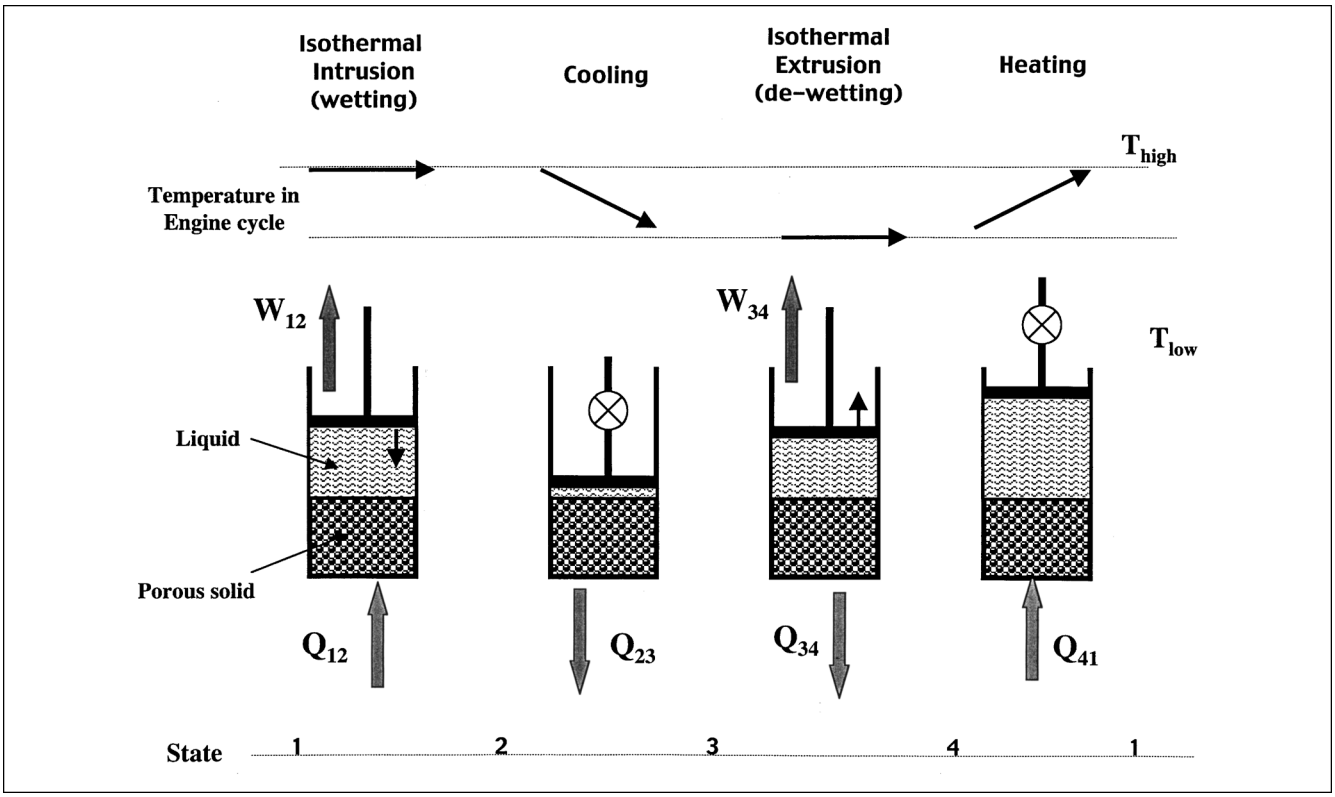

Figure 8. Wetting machine cycles for Cycle C.

Only the engine cycle is feasible. Note the similarity to engine cycle A, except for the work input in the first step.

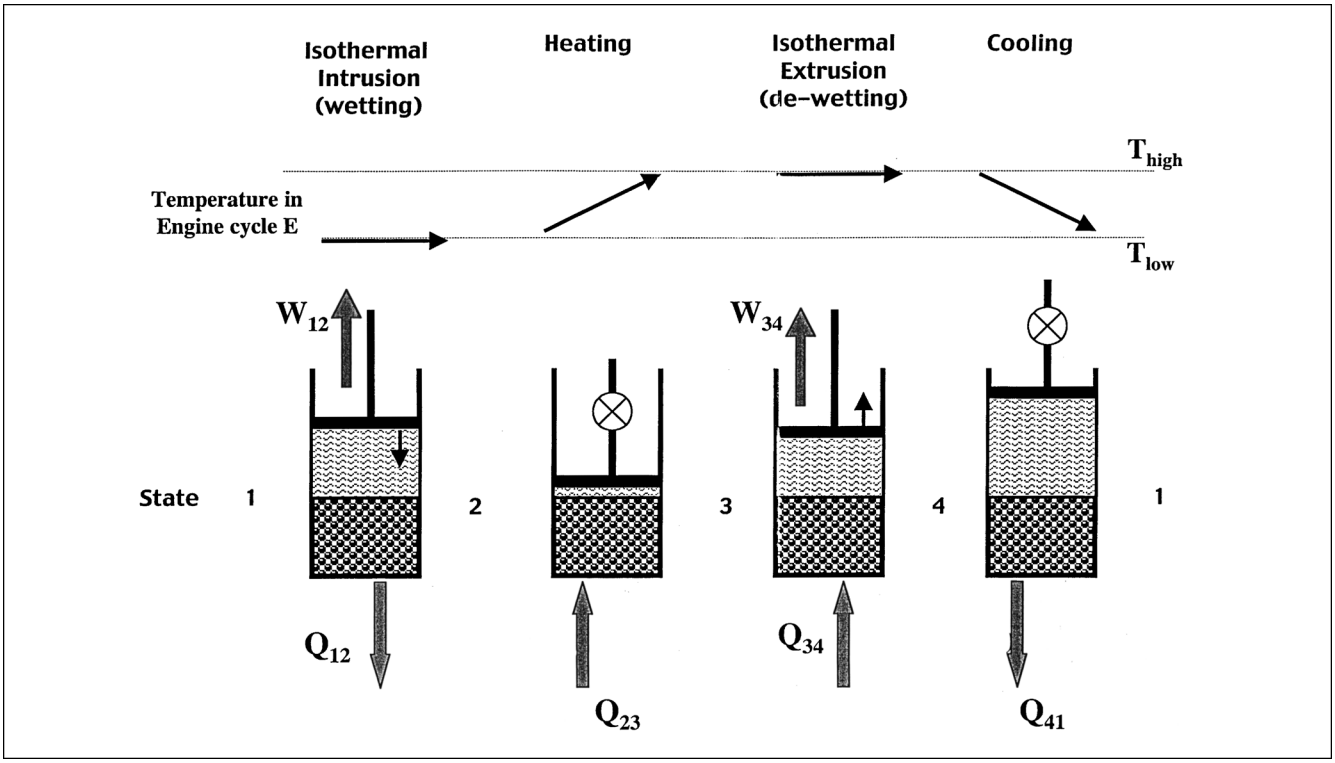

Figure 9. Wetting machine cycles for Cycle D.

Only the engine cycle is feasible. Note the similarity to engine cycle B, except for the work input in the first step.

in mind that the liquid needs to be pushed out of the porous solid in one way or another.

• In Zone 1 (wetting exothermal and exomechanical), the refrigeration/heat pump cycle is possible. On the other hand, the feasibility of an engine cycle faces an unfavorable decrease of θ when switching to dewetting, and will then depend on the variation of the surface tension.

• An engine cycle is possible in Zone 2 (same thermicity and mechanicity as earlier), with a favorable change in θ upon heating to the dewetting step; on the other hand, a refrigeration cycle is submitted to an unfavorable change in θ upon cooling to the dewetting step.

• An engine cycle is possible in Zone 6, with a favorable change in θ, whereas a refrigeration cycle is unfavorable.

We leave it to the reader to analyze the few cases not considered here, and we provide a summary of this compilation in Table 6. As a partial conclusion, we confirm that the basic cycles that we had identified *a priori* and summarized in Table 4 are the most promising, qualitatively speaking:

• Cycle A is the only one to run favorably both ways. Recall that it corresponds to the conditions of Zone 5 for both wetting and dewetting, and to the experimental system water/cholesteryl acetate. Obviously, it is the sort of system we should be looking for.

Table 6. Table of Feasibility of Cycles*

DW Zone ⇒	1		2		3		4		5		6	
W Zone ⇓	E**	R**	E	R	E	R	E	R	E	R	E	R
1	~††	∃‡	∃	∃	+‡‡	~						
2	∃	∃	∃	~	+ +§	X§§				Forbidden		
3	X	~	X	~	+ +	+				cycles†		
4				Forbidden			+	+	~	+	X	~
5				cycles			+	~	+ +	+ +	X	∃
6							+	~	+ +	X		~

*The line index (first vertical column) indicates the zone number for the wetting step, and the column index (first horizontal line) indicates the zone number of the dewetting step.
**E: Engine cycle; R: refrigeration/heat pump cycle.
†The "forbidden cycles" would have two endothermal or two exothermal steps.
††~: Cycle not forbidden, but unpractical or unfavorable.
‡∃: Thermodynamically feasible cycle, but with nonspontaneous dewetting.
‡‡+: Feasible cycle with spontaneous dewetting, but antagonistic change of contact angle.
§+ +: Feasible cycle with spontaneous dewetting, and synergistic change of contact angle.
§§X: Impossible cycle.

• Cycles C and D (with both steps exomechanical) may have some interest for engines, if systems can be found whereby the behavior changes from wetting to nonwetting upon heating (cycle D) or upon cooling (cycle C). They have no corresponding refrigeration cycle.

• Cycle B, which corresponds to our experimental systems of water/hexatriacontane and water/siliconed glass, also works as both direct and reverse cycles, but is qualitatively less favorable than Cycle A.

Discussion of Hypotheses, Simplifications, and Side Effects

Several further important aspects of wetting mechanisms need to be kept in mind, although they are not accounted for in the present approach, and would require attention at a more advanced stage of development. They are hysteresis, nonequilibrium, compressibility and thermal dilatation, force/pressure aspects in relation to materials, chemical aspects such as adsorption, two-dimensional phase changes, and the role of precursor films. Let us give them a brief overview.

Hysteresis of the wetting/dewetting cycles on a *P-V* diagram can have different origins and is relatively well documented (De Gennes, 1985; Chen et al., 1991; Gusev, 1994; Cahn, 2000; Coiffard, 2001), for instance, in relation to mercury porosimetry (Van Brakel et al., 1981; Adamson, 1982). One class of hysteresis relates to the shape of the pores of the solid, particularly the existence of dead-end, ink-bottle-type pores, where the liquid can be trapped. This is to be avoided, and when it occurs, its main effect is to diminish the useful volume of the system. Another class relates to the classic difference between advancing and receding angles of wetting. Although it is essentially due to the geometric or chemical microheterogeneities of the material, it is a practically unavoidable reality. Its effect on an engine cycle might be accounted for in Eq. 31, and would mainly be to diminish the net work. The effect on δQ and on refrigerating cycles is less straightforward and must be examined cycle by cycle. In any case, the use of these quantities in a quasi static approach is questionable.

The existence of a thin "precursor film" (a few atomic layers) that extends well beyond the macroscopic film in the case of a wetting liquid has been ignored here. This questions the meaning and the validity of Young's equation in the case of wetting behavior. For our present purposes, we have chosen to stick to the "classic" view of wetting and to allow for the validity of Young's equation.

We have considered the complete process as reversible both mechanically and thermally. From the mechanical point of view, the rate at which wetting or dewetting occurs determines the power of a real machine, that is, the energy handled per unit time. In fast transformations, viscous dissipation, which may be considerable (De Gennes, 1985; Coiffard, 2001), can no longer be ignored. Even kinetic energy and inertial effects might have to be considered in a rigorous approach. The mechanical aspects of wetting are discussed in detail in the classic paper of De Gennes (1985). From the thermal point of view, the heating and cooling steps are clearly irreversible, even though internal exchange is considered, reducing both the external heat addition and the irreversibility due to transfer across a finite temperature difference. This internal heat compensation must take place between two systems in phase opposition. An additional simplifying assumption concerning heat that is made in the present treatment is to consider the specific heats of the solid/liquid system as the same whether or not they are in contact (compensation of the isochoric heating and cooling steps). Actually, the heat capacity of the impregnated solid can be shown to depend on the second derivative of $\sigma \cos \theta$ with respect to the temperature.

The compressibility and the thermal dilatation of the liquid and/or the solid can entail both reversible and irreversible phenomena. A reversible isothermal pressure change is governed by (Coiffard, 2001)

$$\delta W = -PdV = PV\kappa_T dP \tag{32}$$

$$\delta Q = TdS = -VT\alpha_P dP \tag{33}$$

where κ_T and α_P are, respectively, the isothermal compressibility coefficient and the isobaric dilatation coefficient. From there, it can be shown that for water, the incremental internal energy change dU/dP is of the order of $-0.09\ \mathrm{kJ \cdot MPa^{-1} \cdot kg^{-1}}$, the process being exothermal. This may appear to be a rather small quantity compared to the values encountered in Table 5, but when multiplied by 50 or 100 MPa (see below), it is far from negligible. Furthermore, the ratio $\delta W/\delta Q$ is of the order of -5.10^{-5}, meaning that the internal energy change upon isothermal pressure change is essentially due to heat output. This reversible phenomenon thus seems, for example, to reinforce the exothermal and endomechanical character of cycle B, whereas it would *a priori* tend to weaken the performances of cycle A. Clearly, the irreversible aspects can only be detrimental to any cycle efficiency.

The energy approach taken here completely obliterates the mechanical aspects, which become essential when designing a realistic system. Pressure considerations related to capillary forces must be considered, especially when porous solids are used. The wetting process means intrusion of the liquid into the porosity of the solid; if the behavior is nonwetting ($\cos \theta < 0$), this implies that a high pressure must be applied to force the intrusion, in conformity with Laplace's equation

$$P = -2\sigma \cos \theta / R \tag{34}$$

where R is the pore radius. For example, for $R = 10^{-9}$ m, and mercury as liquid ($\sigma \approx 0.5\ \mathrm{J \cdot m^{-2}}$ and $\theta \approx 140°$ as a typical value in mercury porosimetry; Van Brakel et al., 1981; Leon y Leon, 1998), P is of the order of 760 MPa! For water on cholesteryl acetate ($\sigma \approx 0.07\ \mathrm{J \cdot m^{-2}}$ and $\theta \approx 103°$), P is of the order of 31 MPa, a much more practical value. Measured values for the water–silicalite system (a hydrophobic zeolite) are of the order of 100 MPa, which disagrees with Eq. 34 (Eroshenko et al., 2001, 2002). At these pressure values, two additional aspects have to be discussed: the surface tension decreases when pressure increases (Adamson, 1960), for example, as much as 1 or 2% per MPa, and this effect might be sizable; also, the surface tension decreases when the curvature increases below 100 nm. At 1 nm, the surface

tension may be only 75% of its limit "plane" value (Defay and Prigogine, 1951).

This brings us to the solid materials that can be used and their pore sizes. The value of specific surface Δa, used in the calculation (10^9 $m^2 m^{-3}$) is coherent with classic, but highly porous solid adsorbents (1,000 $m^2 \cdot g^{-1}$) that have a large volume of nanopores ($R \leq 1$ nm), such as activated carbons. We assumed here that the wetting process goes from completely "dry" to completely wetted, and, therefore $\Delta a = a$. Rather, commercial porous silica or zeolites have specific BET surfaces in the range 200 to 400 $m^2 \cdot g^{-1}$. The microporosity of the zeolites ranges from 0.3 nm to 1.5 nm. To observe the behaviors shown in this article, one needs to coat these adsorbents with cholesteryl acetate, silicone, or long-chain alcanes. Techniques for this exist, at least for silica, and are used in manufacturing chromatographic materials, as discussed, for example, by Coiffard (2001).

The extensive work done recently by the latter author should be emphasized, using "scanning transitiometry" (Randzio, 1996), that is, simultaneous calorimetric and mechanical measurements during the intrusion of water into porous silica-based materials made hydrophobic by grafting aliphatic chains. The contact angles are not deduced from these measurements, but from independent BET measurements giving an estimation of pore diameter, and then using the Laplace equation. Unfortunately, measurements were done at a single temperature, and the dependence of the angle on temperature is not obtained. The present authors think that it should be possible to retrieve both θ and $d\theta/dT$ from such experiments by simultaneously solving Eqs. 27 and 29, with measured values of δW and δQ, providing σ and $d\sigma/dT$ are known.

The effects of adsorption, mixture composition, and two-dimensional phase rearrangements can be accounted for in a rigorous formulation of the interfacial thermodynamics, following (Defay and Prigogine, 1951). These aspects may open new perspectives on the present research, and are left for later studies.

Conclusion

The wetting process, or more generally, the extension of an interface between two phases, involves both thermal and mechanical effects, coupled through the dependence of interfacial energies on temperature. In principle, this coupling allows thermal machines that convert heat into mechanical energy (thermal engine) or that pump heat from a cold source (cooling effect) to a hot well (heat pump effect) to be conceived.

The thermodynamics of such systems can be described using adequate state functions (for solid/liquid interfaces considered here, the surface tension of the liquid and the contact angle) and their dependence on temperature.

The thermodynamic and technical feasibility of such machines depends on the details of the thermal behavior of these state functions, and a methodology has been developed to investigate, classify, and select the promising solid/liquid pairs and the feasible cycles. Pairs with nonwetting behavior ($\theta > 90°$) and a negative temperature dependence of the contact angle ($d\theta/dT < 0$), thus showing endothermal and endomechanical wetting and the opposite behavior for dewetting, seem qualitatively the most promising, and can be used for both engine cycles and heat pump/refrigeration cycles. The ideal efficiency of such cycles is the Carnot efficiency, and is, determined by the upper and lower temperature levels of the cycle. The conditions envisaged here, related to the data and the systems available, involving water and some organic liquids, are at near ambient temperatures; the corresponding Carnot efficiency is, therefore, small.

In terms of energy density *per unit mass*, the results are at first sight not very spectacular, as they are more than one order of magnitude lower than systems based on vaporization. On the other hand, since the wetting/dewetting processes occur entirely in the condensed phase, the energy density *per unit volume* is potentially much larger than systems involving gases. This potential compactness is a key point of the interest of surface-based machines. In terms of power, that is energy per unit time, the prospects are less promising: it is unlikely that fast cycles can be used, because they will be limited both by heat transfer and by the kinetics of liquid intrusion/extrusion in the porous medium.

We should also keep in mind that our evaluation is based on ideal machines. Several factors of nonideality are of importance, among which we stress the heat transfer and heat recuperation between the heating and the cooling steps, the viscous dissipation if relatively fast operations are considered, and the hysteresis and the factors that produce it. What the performances of a real system would be seems impossible to predict without experimentation. The conditions under which the confidential 1-kW engine mentioned in the Introduction was built and operated in Russia remain mysterious to us.

In terms of systems, we have restricted our study to simple systems involving water as fluid and working at moderate temperatures. Are there any promising prospects outside this range of conditions? It would be of interest to examine the behavior of mercury as a representative of pure liquid metals. The latter have a very high surface tension, and roughly obey the linear law of variation with temperature (Eq. 8), with a value of α of the same order as mercury, in the vicinity of their melting point (Weast and Astle, 1985). The contact angles are usually high, implying high penetration pressures. The mechanical contribution, δW, to the total energy seems much larger than the heat contribution δQ, and this can lead to the consideration of aspects other than thermal machines.

Obviously, it is interesting to examine the possible engineering design of such machines, if one were to build them. Although this aspect goes beyond the scope of the present work, some thought was given to this question, and also considers the suggestions of Eroshenko (1997). Figure 10 illustrates one possible concept, in which the porous particles (possibly encapsulated) are suspended in the liquid, which is circulated continuously in a circuit involving heat exchangers, compressor, and expansion system.

Is there another point of view from which such systems would be promising? Certainly that of actuators developing a large force: a small amount of work, in the form of a small displacement, but with a strong force, might be of interest in certain machines or tools. Such ideas have already been exploited [Eroshenko (2000), among others]. This approach is closer to mechanical energy storage than to thermal engines. It is analogous to the compression of a spring or a gas, but

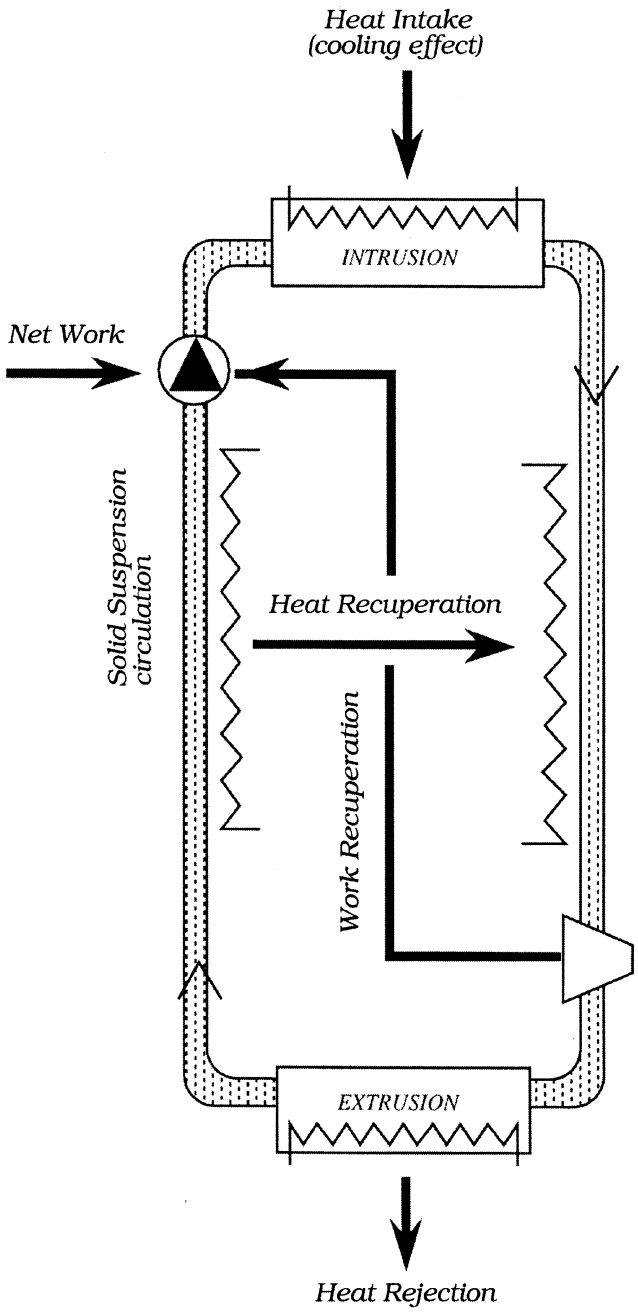

Figure 10. Continuous-flow wetting machine, with the solid carried as a slurry; refrigeration cycle corresponds to Figure 6.

with a much higher capacity for developing force or couple, and the possibility of "regenerating" or recompressing the tool after use by using heat. There may also be some perspectives in simple mechanical energy storage, without thermal conversion. This will be the subject of further studies.

Acknowledgment

The financial support of Electricité de France (Division Recherche et Développement) and the collaboration of Mr. Jean-Louis Grange, of this Division, are gratefully acknowledged. We are thankful to V. Eroshenko (Ecole Polytechnique, Paris-Palaiseau) for providing useful comments, historical information, and a number of references. Finally, we are grateful to Prof. L. Borel of Lausanne for a very careful examination of the manuscript and for numerous suggestions to improve it. While this article was in press, the authors were informed of Sorokin et al. (1998, 1999) concerning developments made in Russia.

Notation

a = specific area of interface, m^{-1}
A = area of interface, m^2
B = parameter in the athermicity curve (Eq. 30), K^{-1}
C = thermal capacity of liquid film, $J \cdot K^{-1}$
C_p = specific heat of bulk liquid, $J \cdot kg^{-1} \cdot K^{-1}$
P = pressure, Pa
Q = heat, thermal energy, J
R = pore radius, m
S = entropy, $J \cdot K^{-1}$
T = temperature, K
U = internal energy, J
V = volume, m^3
W = work, mechanical energy, J

Greek letters

α = thermal coefficient of surface tension, $J \cdot m^{-2} \cdot K^{-1}$ or $N \cdot m^{-1} \cdot K^{-1}$
η = efficiency of thermal engine
Λ = ratio of heat capacity to heat of extension (Eq. 19)
ρ = specific mass of liquid, $kg \cdot m^{-3}$
σ = surface tension of the liquid, $J \cdot m^{-2}$ or $N \cdot m^{-1}$
σ_0 = limit value of surface tension at zero temperature, $J \cdot m^{-2}$ or $N \cdot m^{-1}$
θ = contact angle, Rad

Subscripts

0 = refers to zero temperature
h = refers to the high temperature of a thermodynamic cycle
l = refers to the low temperature of a thermodynamic cycle
i = refers to different interfaces
lg = liquid/gas interface
ls = liquid/solid interface
sg = solid/gas interface

Literature Cited

Adamson, A. W., *Physical Chemistry of Surfaces*, Interscience, New York (1960).
Bernardin, J. D., I. Mudawar, C. B. Walsh, and E. Franses, "Contact Angle Temperature Dependence for Water Droplets on Practical Aluminum Surfaces," *Int. J. Heat Mass Transfer*, **40**, 1017 (1997).
Briant, J., *Phénomènes d'Interface Agents de Surface*, Editions Technip, Paris (1989).
Cahn, J. W., "Wetting and Non-Wetting Near Critical Points in Solids," *Physica A*, **279**, 195 (2000).
Chen, Y. L., C. A. Helm, and J. N. Israelachvili, "Molecular Mechanisms Associated with Adhesion and Contact Angle Hysteresis of Monolayer Surfaces," *J. Phys. Chem.*, **95**, 10736 (1991).
Coiffard, L., "Etude des Systèmes Hétérogènes Lyophobes Matrice Poreuse–Liquide. Elucidation de la Nature de l'Hystérésis dans les Processus Isothermes Compression/Détente à l'Aide de la Transitiométrie à Balayage," PhD Thesis, Univ. Blaise Pascal, Clermont-Ferrand, France (2001).
Defay, R., and I. Prigogine, *Tension Superficielle et Adsorption*, Dunod, Paris (1951).
De Gennes, P. G., "Wetting: Statics and Dynamics," *Rev. Mod. Phys.*, **57**, 827 (1985).
De Ruijter, M., P. Kölsc, M. Voué, J. de Conninck, and J. P. Rabe, "Effect of Temperature on the Dynamic Contact Angle," *Colloids Surf. A: Physicochem. Eng. Aspects*, **144**, 235 (1998).
Eötvös, R. V., *Wied. Ann.*, **27**, 456 (1886).
Eroshenko, V. A., "Heterogeneous Thermodynamical System, Eroshenko Cycle of Transformation of Thermal Energy into Me-

chanical Energy and Devices to Achieve It," (in Russian), Soviet Patent No. 1,254,811 (1981) [priority of 24.07.1981, updated 02.09.1993 (date of free public access)].
Eroshenko, V. A., Russian-Soviet Patents No. 943,444 (1980), 1,382,078 (1982), 1,380,357 (1983), 1,333,870 (1985), 1,434,881 (1985), 1,452,262 (1986), 1,508,665 (1987).
Eroshenko, V. A., "Effect of Heat Exchange on Filling of Lyophobic Pores and Capillaries with Liquid," *Kolloidn. Zh.*, **49**, 875 (1987).
Eroshenko, V. A., "Les propriétés Non-Ordinaires d'un Système Thermodynamique Complexe," *C. R. Acad. Sci. Ukraine, Ser. A*, **10**, 79 (1990).
Eroshenko, V. A., and A. Y. Fadeev, "Intrusion and Extrusion of Water in Hydrophobized Porous Silica," *Colloid J.*, **57**, 4, 446 (1995).
Eroshenko, V. A., "Dimensionnalité de l'Espace Comme Potentiel Thermodynamique d'un Système," Entropie, **202**, 110 (1997).
Eroshenko, V. A., "Non-Compressibilité et Non-Dilatabilité Adiabatiques d'un Système Thermodynamique Complexe," *Entropie*, **196**, 17 (1996).
Eroshenko, V. A., "Amortisseur à Haut Pouvoir Dissipatif," French Patent No. FR 2 804 188 A1 (2000).
Eroshenko, V. A., R.-C. Regis, M. Soulard, and J. Patarin, "Energetics: A New Field of Applications for Hydrophobic Zeolites," *J. Am. Chem. Soc.*, **123**, 8129 (2001).
Eroshenko, V. A., R.-C. Regis, M. Soulard, and J. Patarin, "Les Systèmes Hétérogènes Eau-Zéolithe Hydrophobe: De Nouveaux Ressorts Moléculaires," *C. R. Acad. Sci., Ser. B*, **3**, 111 (2002).
Fadeev, A. Y., and V. A. Eroshenko, "Study of Penetration of Water into Hydrophobized Porous Silica," *J. Colloid Interface Sci.*, **187**, 275 (1997).
Gomez, F., R. Denoyel, and J. Rouquerol, "Determining the Contact Angle of a Non-Wetting Liquid in Pores by Liquid Intrusion Calorimetry," *Langmuir*, **16**, 4374 (2000).
Good, R. J., and C. H. Yu, "A New Observation in Surface Chemistry: The Variation of Liquid-Solid-Gas Contact Angle with Change in Gas Pressure," *Colloids Surf. A: Physicochem. Eng. Aspects*, **186**, 17 (2001).
Guggenheim, E. A., *J. Chem. Phys.*, **13**, 253 (1945).
Gusev, V. Y., "On Thermodynamics of Permanent Hysteresis in Capillary Lyophobic Systems and Interface Characterization," *Langmuir*, **10**, 235 (1994).
Hansen, G., A. A. Hamouda, and R. Denoyel, "The Effect of Pressure on Contact Angles and Wettability in the Mica/Water/*n*-Decane System and the Calcite + Stearic Acid/Water/n-Decane System," *Colloids Surf. A: Physicochem. Eng. Aspects*, **172**, 7 (2000).
Jasper, J. J., *J. Phys. Chem. Ref. Data*, **1**, 841 (1972).
Leon y Leon, C. A., "New Perspectives in Mercury Porosimetry," *Adv. Colloid Interface Sci.*, **76-77**, 341 (1998).
Moelwyn-Hughes, E. A., *Physical Chemistry*, Pergamon Press, New York (1951).
Neumann, A. W., "Contact Angles and Their Temperature Dependence: Thermodynamic Status, Measurement Interpretation and Application," *Adv. Colloid Interface Sci.*, **4**, 105 (1974).
Pepin, X., S. Blanchon, and G. Couarraze, "Powder Dynamic Contact Angle Measurements: Young Contact Angles and Effectively Wet Perimeters," *Powder Technol.*, **99**, 264 (1998).
Perry, R. H., and D. W. Green, *Perry's Chemical Engineers Handbook*, 7th ed., Chap. 2, McGraw-Hill, New York, p. 372 (1998).
Randzio, S. L., "Scanning Transitiometry," *Chem. Soc. Rev.*, **25**, 383 (1996).
Reid, R. C., J. M. Prausnitz, and B. E. Poling, *The Properties of Gases and Liquids*, McGraw-Hill, New York (1987).
Rouquerol, F., J. Rouquerol, and K. Singh, *Adsorption by Powders and Porous Solids*, Chap. 5, Academic Press, London (1999).
Rowlinson, J. S., and B. Widom, *Molecular Theory of Capillarity*, Clarendon Press, Oxford (1982).
Sorokin, A. P., V. S. Egorov, A. G. Portyanoy, and E. N. Serdun, "Hydrocapillary Thermal to Electric Energy Conversion Device," Space Technology and Applications International Forum (STAIF-98), Albuquerque, NM, 1621 (Jan. 24-25, 1998).
Sorokin, A. P., A. G. Portyanoy, and E. N. Serdun, "Development of Power Devices Based on Lypophobous Working Bodies," Space Technology and Applications International Forum (STAIF-99), Albuquerque, NM (Jan. 31-Feb. 4, 1999).
Stefan, J., "Über die Beziehung zwischen den Theorien der Kapillarität und der Verdampfung," *Anal. Phys. Chem.*, **29**, 655 (1886).
Sudgen, S., *The Parachor and Valency*, Routbadge, London (1930).
Thomson, W., *Philos. Mag.*, **4**, 61 (1859).
Van Brakel, J., S. Modry, and M. Svata, "Mercury Porosimetry: State of the Art," *Powder Technol.*, **29**, 1 (1981).
Vold, R. D., and M. J. Vold, *Colloid and Interface Chemistry*, Addison-Wesley, Reading, MA (1983).
Weast, R. C., and M. J. Astle, *Handbook of Chemistry and Physics*, 66th ed., CRC Press, Boca Raton, FL (1985).
Young, T., *Philos. Trans. Roy. Soc. London*, **95**, 65 (1805).
Zisman, W. A., "Relation of Equilibrium Contact Angle to Liquid and Solid Constitution," F. M. Fowkes and R. F. Gould, eds., *Contact Angle Wettability and Adhesion, Advances in Chemistry Series*, Vol. 43, American Chemical Society, Washington, DC, p. 1 (1964).

Appendix A: Contact Angles as Functions of Temperature

This Appendix is based on Neumann (1974). The data were obtained by measurements of the capillary rise at a vertical plate. No hysteresis was observed (Figures A1 and A2).

The "accident" around 60°C in Figure A2 is correlated to the solid/solid phase transition observed on differential thermal analysis curves, and is probably due to an impurity. The melting point is at about 70°C.

The accident around 40°C in Figure A3 is due to a solid/solid phase transition observed also on DTA curves. The melting point is about 117°C.

Appendix B: Derivation of Eq. 6

We start from Eq. 5

$$(\partial T/\partial A)_S = (\partial \sigma/\partial S)_A \tag{B1}$$

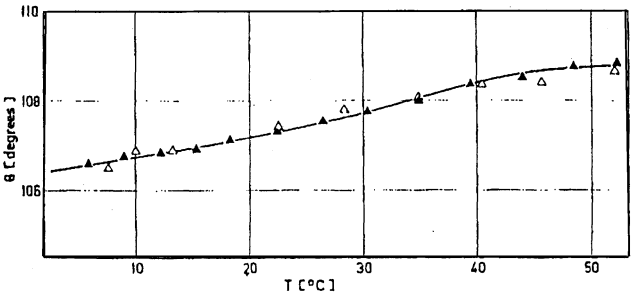

Figure A1. Water on siliconed glass (measured by the vertical plate technique).

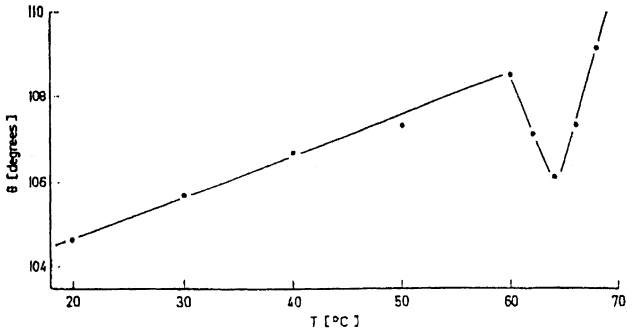

Figure A2. Water on hexatriacontane (obtained from capillary rise measurements).

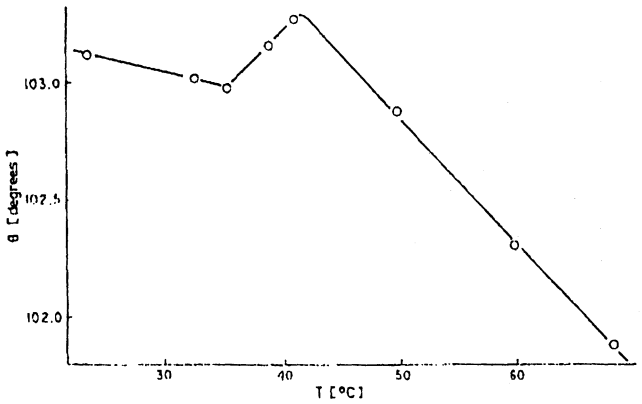

Figure A3. Water on cholesteryl acetate.

where S is a function of T and A, and σ is a function of T alone, so that we can write the partial derivative of the right-hand side as

$$(\partial\sigma/\partial S)_A = d\sigma/dT(\partial T/\partial S)_A \tag{B2}$$

The chain rule between the variables T, A, and S is written as

$$(\partial T/\partial A)_S(\partial A/\partial S)_T(\partial S/\partial T)_A = -1 \tag{B3}$$

so that

$$(\partial T/\partial A)_S/(\partial T/\partial S)_A = -1/(\partial A/\partial S)_T = -(\partial S/\partial A)_T \tag{B4}$$

Now substitute Eq. B2 into Eq. B1 and use Eq. B4 to eliminate the partial derivatives of T, to obtain

$$d\sigma/dT = -(\partial S/\partial A)_T \tag{B5}$$

For an isothermal transformation, one can write formally

$$(\partial S/\partial A)_T = dS/dA \tag{B6}$$

and Eq. 6 results immediately.

Manuscript received Feb. 25, 2002, and revision received Sept. 12, 2002.